RSC Advances

PAPER

View Article Online
View Journal | View Issue

Check for updates

Cite this: *RSC Adv.*, 2022, **12**, 19022

Rapid preparation of N-CNTs/P(AA-*co*-AM) composite hydrogel *via* frontal polymerization and its mechanical and conductive properties

Bin Li, *[a] Xiaojia Xu,[a] Zhigang Hu,[a] Yongjing Li,[b] Mengjing Zhou,[a] Jizhen Liu,[a] Yajun Jiang[a] and Peng Wang[c]

Received 28th March 2022
Accepted 16th May 2022

DOI: 10.1039/d2ra02003c

rsc.li/rsc-advances

Deep eutectic solvent (DES) was prepared by using acrylic acid (AA) and acrylamide (AM) as hydrogen bonding donors (HBD) and choline chloride (ChCl) as hydrogen bonding receptors (HBA). Nitrogen-doped carbon nanotubes (N-CNTs) were dispersed in DES as fillers, and N-CNTs/P(AA-*co*-AM) composite hydrogels were prepared by FP. The interaction mode between the hydrogel and N-CNTs was characterized by Fourier infrared spectroscopy (FTIR) and scanning electron microscopy (SEM). The mechanical properties, pH response and electrical conductivity of the composite hydrogels were studied. The results showed that the mechanical properties of the hydrogel were significantly enhanced with the increase of N-CNT content. The tensile strength and compressive strength of the FP4 composite hydrogel reached 5.42 MPa and 4.29 MPa, respectively. Due to the dissociation of carboxyl groups in AA in an alkaline environment the composite hydrogel showed excellent pH response performance. The conductivity of the hydrogel was also found to be improved with the content of N-CNTs. When the content of N-CNTs is 1.0 wt%, the conductivity of the hydrogel was 4.2 times higher than that of the hydrogel without N-CNTs, and connecting it to a circuit can make an LED lamp emit bright light. In this study, a simple and green method was proposed to prepare composite hydrogels with excellent mechanical properties and electrical conductivity by FP of DES in less than 5 min.

Open Access Article. Published on 29 June 2022. Downloaded on 2/6/2026 6:33:03 AM.
This article is licensed under a Creative Commons Attribution-NonCommercial 3.0 Unported Licence.

1. Introduction

Hydrogels are polymers with a three-dimensional network structure, and have wide application in drug delivery systems,[1] artificial muscle,[2] sensors,[3] biomaterials,[4] electrochemical biosensors[5] and so on. Nowadays, with the development of environment-friendly flexible conductive materials, hydrogels with good mechanical properties and high conductivity are getting more and more attention.[6,7] Conductive hydrogels can be divided into polyelectrolyte conductive hydrogels,[8,9] acid-doped conductive hydrogels,[10,11] inorganic conductive hydrogels[12,13] and conductive polymer-based conductive hydrogels.[14,15] The mechanical strength and stability of single polyelectrolyte conductive hydrogels are not satisfactory. On the other hand, the conductive hydrogels with inorganic additives or conductive polymer materials show good conductivity and good mechanical strength, and show higher practical application value.[16,17]

As a conductive polymer material, carbon nanotubes (CNTs) have high aspect ratio, high strength, excellent mechanical and electrical properties,[18] and can be used to prepare high strength composites and electrical functional materials.[19,20] By replacing the carbon atoms on the CNTs' six-membered ring skeleton with nitrogen atoms, a free electron is provided as a carrier for the fermi layer of carbon nanotubes, and nitrogen-doped carbon nanotubes (N-CNTs) with better electrical properties are formed.[21] In addition, N-CNTs have good dispersion properties and can be uniformly dispersed in the polymer matrix, which opens a new way for its application in the electronic field.[22]

Compared with other methods of preparing polymers, frontal polymerization (FP) is a new type of polymerization, its principle is to convert low molecular weight monomers into high molecular weight polymers through the local reaction region,[23] which has the advantages of short reaction time and good self-propagation. Compared with traditional polymerization, the self-propagating property of FP reduces the energy cost of polymer preparation and provides high conversion in a shorter reaction time.[24] Deep eutectic solvent (DES) is a new type of ionic liquid solvent composed of two or more components at its eutectic point, consisting of hydrogen-bonded receptors (HBA, such as quaternary ammonium salts, alkyl ammonium salts, *etc.*) and hydrogen-bonded donors (HBD,

[a]*School of Mechanical Engineering, Wuhan Polytechnic University, Wuhan, Hubei 430023, China. E-mail: lb420@whpu.edu.cn*

[b]*Hubei Key Laboratory of Theory and Application of Advanced Materials Mechanics, Wuhan University of Technology, Wuhan, Hubei 430070, China*

[c]*Wuhan Second Ship Design and Research Institute, Wuhan, 430205, China*

© 2022 The Author(s). Published by the Royal Society of Chemistry

Open Access Article. Published on 29 June 2022. Downloaded on 2/6/2026 6:33:03 AM.
This article is licensed under a Creative Commons Attribution-NonCommercial 3.0 Unported Licence.

such as acids, amides and alcohols, *etc.*).[25,26] As a reaction solvent, DES can reduce the use of toxic organic solvents and reduce environmental pollution.[27] At the same time, DES has the advantages of low cost, low volatility, recyclability and good biocompatibility,[28,29] which can provide effective help for the self-propagating characteristics of FP.

At present, there are few studies on the preparation of conductive hydrogels by FP. On the basis of previous studies,[30] we prepared N-CNTs/P(AA-*co*-AM) composite hydrogels with good conductivity in DES by FP, and studied the effect of N-CNTs content on the related properties of the composite hydrogels. Using acrylic acid (AA) and acrylamide (AM) as HBD, choline chloride (ChCl) as HBA. These three raw materials were heated and mixed at 1 : 1 : 1, and the polymerizable DES was obtained. Then different mass fractions of N-CNTs were added and heated in the test tube to get N-CNTs/P(AA-*co*-AM) hydrogel. The composite hydrogels were characterized by Fourier infrared spectroscopy (FTIR) and scanning electron microscopy (SEM). The effects of different contents of N-CNTs on the mechanical properties, pH response and electrical conductivity of the composite hydrogels were studied.

2. Materials and methods

2.1 Materials

Choline chloride (ChCl), acrylic acid (AA) and acrylamide (AM) were purchased from Shanghai Aladdin biochemical Technology Co., Ltd; potassium persulfate (KPS) was purchased from National Pharmaceutical Group Chemical Reagent Co., Ltd; *N*-methylene bisacrylamide (MBA), citric acid, sodium citrate, sodium carbonate and sodium bicarbonate were purchased from Tianjin Komeo Chemical Reagent Co., Ltd. Nitrogen-doped carbon nanotubes (N-CNTs), 10–30 μm in length and 30–50 nm in diameter, were purchased from Hangzhou Hangdan Optoelectronic Technology Co., Ltd. All raw materials are analytically pure and directly used without purification. ChCl needs to be vacuum dried at 80 °C for two hours to remove moisture before use.

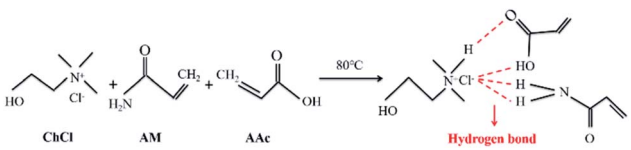

Fig. 1 The formation equation of DES.

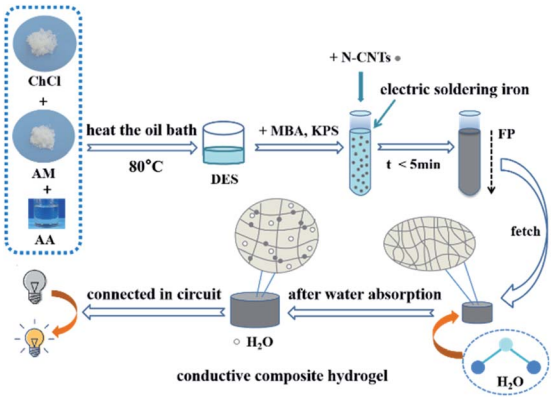

Fig. 2 Preparation schematic diagram of composite hydrogel.

2.2 Preparation of DES

AA and AM were selected as HBD, ChCl was selected as HBA. These three kinds of raw materials were mixed in a beaker with a molar ratio of 1 : 1 : 1, and heated and stirred in an oil bath at 80 °C until the liquid become clear and transparent, and the polymerizable DES was obtained. Then different contents of N-CNTs were added to DES and stirred sufficiently to make it uniformly dispersed in DES to obtain DES/N-CNTs mixed solution. The formation equation of DES is shown in Fig. 1.

2.3 FP of the mixture of DES and DES/N-CNTs

The cross-linking agent (MBA) and initiator (KPS) were mixed into DES/N-CNTs solution with different N-CNTs content, the specific content of each composition for different samples were given in Table 1. The solution was poured into a test tube with a diameter of 12 mm and a length of 100 mm after stir. An electric iron was used to trigger a liquid front at the top of the test tube for FP. When the polymerization front moved to the end of the reaction at the bottom of the test tube, the hydrogel was taken out and set aside. The FP preparation flow chart was shown in Fig. 2.

2.4 Determination of front-end movement rate and temperature

Frontal polymerization generally has a constant front-end moving speed, which can be determined by measuring the relationship between the front-end position changes and times. Before the reaction, the K-type thermocouple was inserted into the 70 mm under the liquid surface and the top of the liquid surface was triggered by an electric soldering iron. Once the

Table 1 The composition of FP samples

Samples	ChCl (g)	ChCl (g)	ChCl (g)	KPS (wt%)	MBA (wt%)	N-CNTs (wt%)	V_f (cm min^{-1})	T_{max} (°C)
FP0	4.189	2.162	2.132	0.3	1.0	0	1.92	152.9
FP1	4.189	2.162	2.132	0.3	1.0	0.2	2.18	156.6
FP2	4.189	2.162	2.132	0.3	1.0	0.3	2.40	157.4
FP3	4.189	2.162	2.132	0.3	1.0	0.5	2.80	158.4
FP4	4.189	2.162	2.132	0.3	1.0	1.0	3.00	163.3

© 2022 The Author(s). Published by the Royal Society of Chemistry

Open Access Article. Published on 29 June 2022. Downloaded on 2/6/2026 6:33:03 AM.
This article is licensed under a Creative Commons Attribution-NonCommercial 3.0 Unported Licence.

front-end front was formed, the temperature was recorded, and the relation curve between the front position and temperature can be obtained. The front-end moving speed and maximum temperature for each sample were given in Table 1.

2.5 Characterization and performance test of hydrogels

The prepared polymer samples were cut into 1–3 mm thick columnar slices, and soaked in distilled water for 7 days. Soluble substances were removed from the sample, it was then pre-frozen and dried to constant weight in a vacuum freeze dryer at −60 °C. After taking out the dry hydrogel sample for grinding, the spectral characteristics of the hydrogel samples were analyzed by FTIR between the wavenumber 500–4000 cm^{-1}; the internal phase state was observed by SEM; the tensile properties of the hydrogel sample were tested on an electronic universal testing machine controlled by a microcomputer, the original standard distance was 50 mm and the tensile speed was 100 mm min^{-1}. The compression property of the hydrogel was tested by TA.XTC-18 texture analyzer, the compression speed was 0.2 mm s^{-1} and the deformation was 80%. The pH responsiveness of hydrogels was studied by preparing buffer solutions with pH of 3, 4.8 (citric acid/sodium citrate) and pH of 9.4, 10.8 (sodium carbonate/sodium bicarbonate). The acidity and alkalinity of hydrogels were accurately detected by digital pen acidity meter (PH208, accuracy 0.01). The swelling property of the hydrogel was tested by gravimetric analysis, the dry hydrogel was soaked in the prepared buffer solution, the hydrogel was removed at regular intervals. The water on the surface was dried with filter paper, and the swollen hydrogel was weighed until the weight of the hydrogel was no longer changed. The resistance of the columnar hydrogel sample was measured by the double electrode method, the resistance change of the sample was tested within 30 hours at room temperature, and then the conductivity was calculated according to formula (3).

The calculation formulas of tensile strength and compressive strength of materials were as follows:

$$P = \frac{F}{S} \quad (1)$$

where, F is the applied force, unit N; S is the cross-sectional area of hydrogel, unit m^2.

The formula for calculating the swelling rate was as follows:

$$\mathrm{ESR} = \frac{W_t - W_0}{W_0} \quad (2)$$

where, W_t is the weight of hydrogel after swelling at t time, and W_0 is the weight of xerogel before swelling.

The calculation formula of ionic conductivity was as follows:

$$\sigma = \frac{1}{R}\frac{d}{S} \quad (3)$$

where, the conductivity is expressed by the greek letter σ, unit mS cm^{-1}; d is the thickness of the hydrogel, unit cm; S is the cross-sectional area of the hydrogel, unit cm^2; R is the tested resistance, unit Ω.

3. Results and discussion

3.1 Frontal velocity and temperature measurement

There was an obvious interface between the polymer and the mixture of unreacted monomers during the frontal polymerization, which was called the front-end front. As shown in Fig. 3(a), the front-end position had a good linear relationship with time, and the FP can be completed quickly in less than 5 min. The preparation time of the five groups of hydrogels was 4.2 min, 3.6 min, 3.3 min 2.8 min and 2.6 min, respectively. At the same time, from the relationship between the position of the front end of the hydrogel and time, it can be seen that the moving speed of the front end of the polymerization was uniform, which proved that there was no self-polymerization in the FP reaction.[31] With the increase of N-CNTs content, the front-end reaction rate increases, and when the N-CNTs content increased from 0 wt% to 1.0 wt%, V_f (frontal velocity) increases from 1.92 cm min^{-1} to 3.00 cm min^{-1}. The relationship between the front position of the hydrogel and temperature was

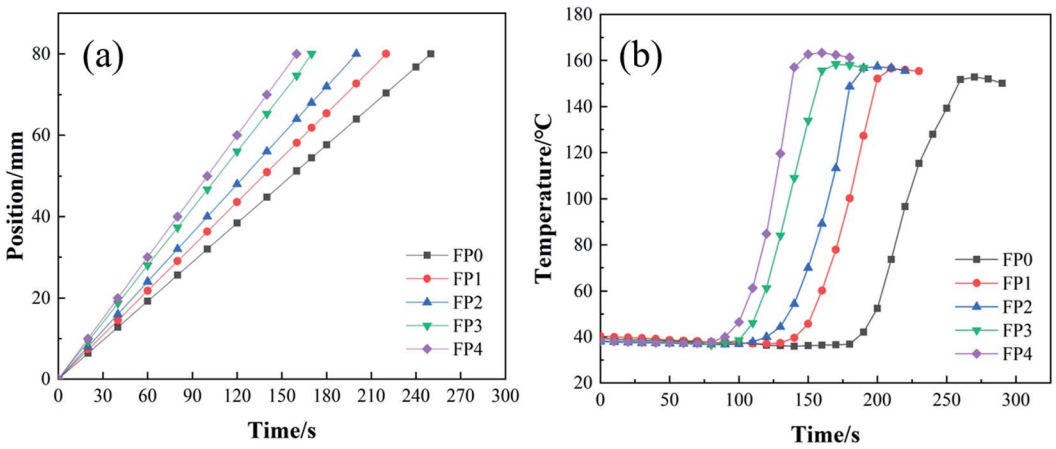

Fig. 3 (a) Variation of the position of the front end of the hydrogel with time; (b) the relationship between the position of the front end of the hydrogel and the temperature.

© 2022 The Author(s). Published by the Royal Society of Chemistry

Open Access Article. Published on 29 June 2022. Downloaded on 2/6/2026 6:33:03 AM.
This article is licensed under a Creative Commons Attribution-NonCommercial 3.0 Unported Licence.

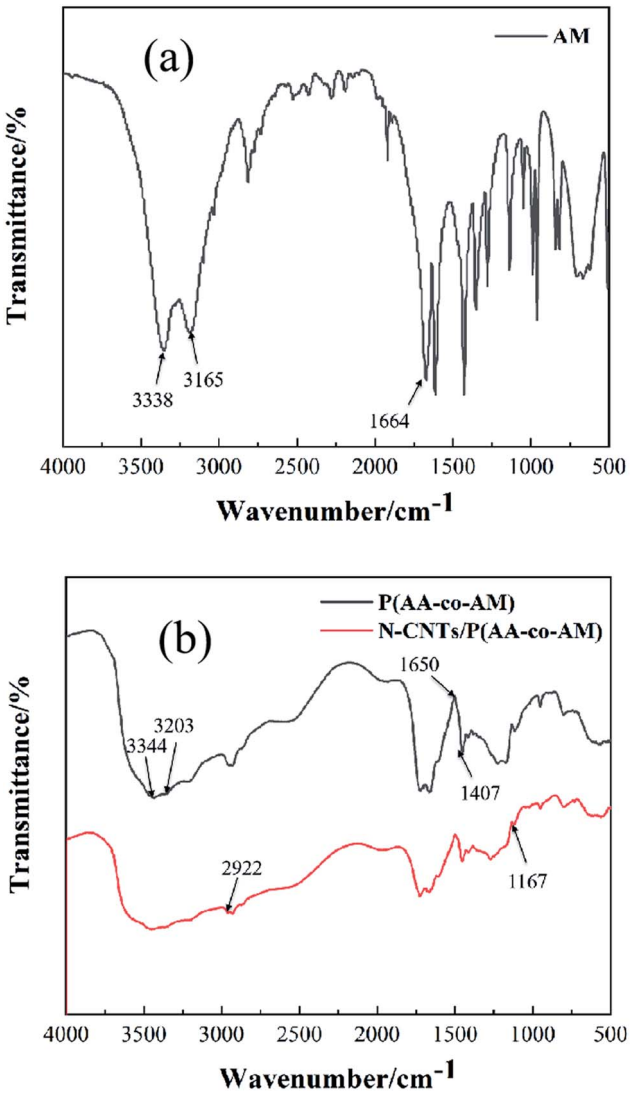

Fig. 4 (a) FTIR diagram of AM; (b) FTIR diagram of FP0, FP4 and N-CNTs.

shown in Fig. 3(b). After the addition of N-CNTs, the maximum temperature of the reaction increased significantly from 152.9 °C to 163.3 °C, because N-CNTs acted as a cross-linking agent, which increased the liquid viscosity of the mixture, resulting in a higher frontier temperature.[32]

3.2 FTIR spectrum and SEM scanning of hydrogels

The infrared spectra of AM, FP0, FP4 and N-CNTs were analyzed, and the results were shown in Fig. 4. As illustrated in Fig. 4(a), the absorption peak at 3338 cm^{-1} and 3165 cm^{-1} was attributed to the stretching vibration peak of $-NH_2$ on the amide groups ($-CONH_2$) in AM, while the absorption peak at 1664 cm^{-1} was the stretching vibration peak of C=O and the vibration peak of C=C.[33] It can be seen from Fig. 4(b) that FP0 had a strong absorption band of $-CONH_2$ at 3344 cm^{-1} and 3203 cm^{-1}, which corresponded to the stretching vibration peak of $-NH_2$ at 3338 cm^{-1} and 3165 cm^{-1} in AM.[34] The absorption peak at 1650 cm^{-1} was the stretching vibration peak of the binding of C=O in AM amide group to C=O in AA carboxyl anion $-COO^-$.[35] 1407 cm^{-1} was the characteristic peak of C=O on the carboxyl salts of AA. The intensity of the absorption peak of pure N-CNTs was very weak, and there was no obvious peak compared with the infrared spectra of the other two hydrogels. From the infrared spectrum curve of FP4, it could be seen that the absorption peak of FP4 was almost the same as that of FP0, but FP4 added some functional groups on the basis of FP0. The symmetric stretching vibration peak of C–H in N-CNTs was at 2922 cm^{-1}, and the stretching vibration peak of C–O in N-CNTs was at 1167 cm^{-1}.[36] To sum up, the copolymerization of AA and AM took place first, and the N-CNTs molecule entered the hydrogel network after the polymerization.

In order to study the distribution of N-CNTs in the hydrogel matrix, five groups of FP0–FP4 hydrogels and pure N-CNTs were analyzed by SEM. Before SEM test, the target hydrogel was pre-frozen, then freeze-dried in a vacuum freeze dryer for 48 hours. Fig. 5 showed scanning electron microscopic images of the internal sections of five groups of hydrogels. It could be seen from Fig. 5(a) that the surface of P(AA-*co*-AM) without N-CNTs was smooth. Fig. 5(b) indicated that when the content of N-CNTs was 0.2 wt%, the dispersion of N-CNTs was relatively uniform, while Fig. 5(c) showed that when the content of N-CNTs is 0.3 wt%, there was a small amount of agglomeration in the polymer matrix. But it could be seen from Fig. 5(d) and (e), the size of agglomeration increased gradually when the content of N-CNTs were 0.5 wt% and 1 wt%. This may be because the viscosity of the mixture increased with the increase of N-CNTs content, which made N-CNTs agglomerate in the polymer matrix, resulting in the incomplete dispersion of N-CNTs.[37]

3.3 Mechanical properties of hydrogel

The test of tensile properties of hydrogels were shown in Fig. 6(a). It could be seen from the figure that the maximum

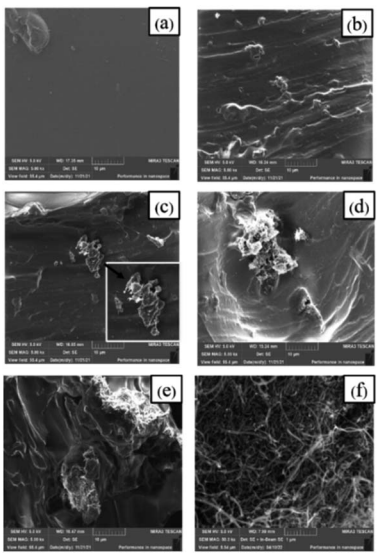

Fig. 5 SEM diagram of FP0 (a), FP1 (b), FP2 (c), FP3 (d), FP4 (e) and N-CNTs (f).

Open Access Article. Published on 29 June 2022. Downloaded on 2/6/2026 6:33:03 AM.
This article is licensed under a Creative Commons Attribution-NonCommercial 3.0 Unported Licence.

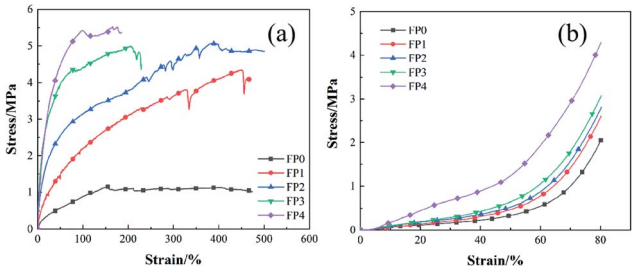

Fig. 6 (a) Test curve of tensile properties of hydrogel; (b) test curve of compressive properties of hydrogel.

tensile strength of FP1–FP4 hydrogel were 3.77, 4.25, 4.30 and 4.71 times higher than that of FP0 hydrogel (the maximum tensile strength was 1.15 MPa). Fig. 6(b) showed the compressive stress–strain curves of five groups of hydrogels. The maximum compressive strength of FP0, FP1, FP2, FP3 and FP4 hydrogels were 2.06(±0.02) MPa, 2.6(±0.01) MPa, 2.8(±0.03) MPa, 3.07(±0.02) MPa and 4.29(±0.01) MPa, respectively. It could be seen that the tensile/compressive strength of the composite hydrogel increased significantly with the increase of N-CNTs content, especially the FP3 and FP4 samples. The enhancement degree of N-CNTs on the mechanical properties of hydrogel depended on the interaction between N-CNTs and polymer.[38] This was because N-CNTs had good hydrophobic properties and can form a denser network structure.[32] At the same time, there were –OH and –COOH on the surface of N-CNTs, which could form a strong interface connection with macromolecules through C–O–C chemical bond in AA free radical polymerization system. The interface connection made the hydrogel play the role of load transfer when subjected to external forces, and the load transfer was one of the important mechanisms to enhance the mechanical

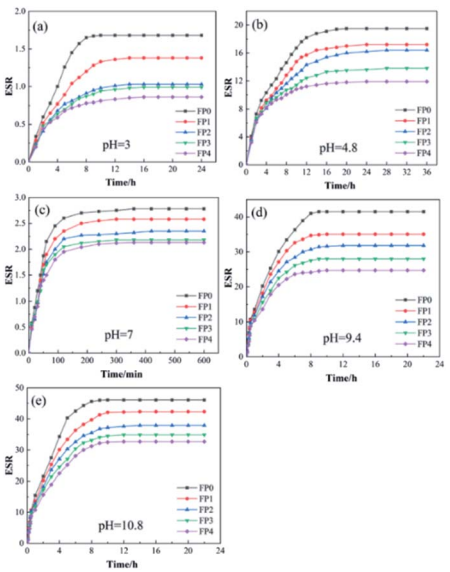

Fig. 7 Swelling kinetics curve (a) pH = 3; (b) pH = 4.8; (c) pH = 7; (d) pH = 9.4; (e) pH = 10.8.

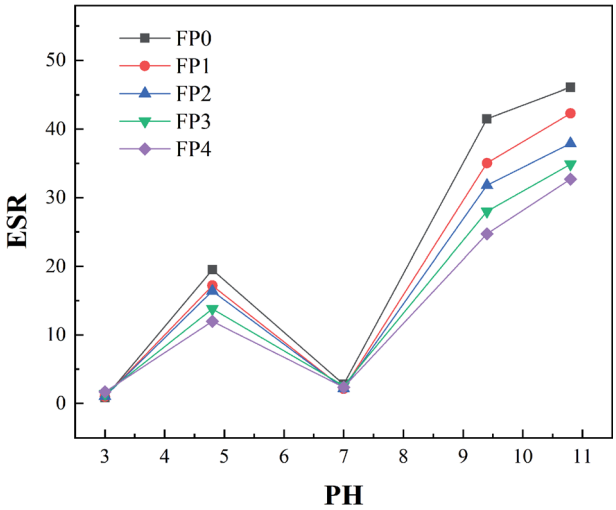

Fig. 8 pH response curve of hydrogels.

properties of polymer composites.[39] When the hydrogel matrix was subjected to external load, the load was transferred to N-CNTs with higher mechanical properties through the interface, which enhanced the mechanical properties of the gel network.[40]

3.4 pH responsiveness of hydrogels

The swelling kinetics curve of the hydrogel was shown in Fig. 7. It could be seen from the figure that the swelling equilibrium of the composite hydrogel decreases with the increase of N-CNTs content. This was due to the fact that the addition of N-CNTs promoted the physical entanglement of long chains of macromolecules, which led to the increase of cross-linking density and thus reduced the swelling properties of the hydrogels.

Fig. 8 showed the swelling behavior of five groups of hydrogels at different pH values. It could be seen from the diagram that the change trend of swelling properties of N-CNTs hydrogels with different contents was basically the same with the increase of pH value. Under the condition of strong acid, due to the hydrogen bond interaction between –COOH on the polymer chain, the polymer chain in the whole network was entangled with each other and contracted, resulting in a low ESR. In the range of 3–4.8 for pH, the hydrogen bonding interaction between –COOH groups was obviously weakened and the electrostatic repulsion was gradually enhanced,[41] which led to an upward trend for ESR. However, most of the –COOH and $–CONH_2$ groups exist in non-ionized form when pH reaches 4.8, the hydrogen bonding between the two groups may lead to cross-linking and sharply reduced the swelling ratio of the hydrogel.[41] The drastic change of swelling behavior near pH 7 may be due to the increase of cross-linking density. The growth density was induced by the intermolecular hydrogen bond between $–CONH_2$ groups and the hydrogen bond interaction with carboxylic acid groups, resulting in the shrinkage of the hydrogel network.[42] Under alkaline conditions, due to the ionization effect of carboxylic acid, –COOH dissociated into $–COO^-$, and the electrostatic repulsion between ions drived the

© 2022 The Author(s). Published by the Royal Society of Chemistry

Open Access Article. Published on 29 June 2022. Downloaded on 2/6/2026 6:33:03 AM.
This article is licensed under a Creative Commons Attribution-NonCommercial 3.0 Unported Licence.

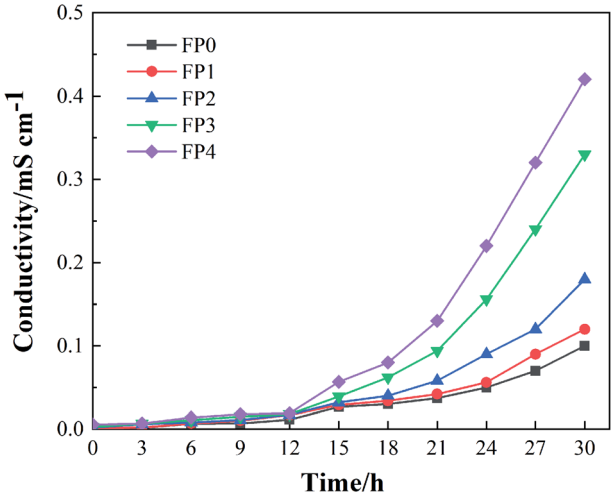

Fig. 9 Conductivity of FP0, FP1, FP2, FP3 and FP4 hydrogels at different time.

polymer chain to diffuse, resulting in more space for water molecules in the hydrogel and an increase in ESR.[43] However, with the increase of N-CNTs content, the ESR of hydrogel decreased gradually, which may be due to the fact that a large number of –OH and –COOH were produced on the surface of hydrogel after adding N-CNTs, which increased the force between polymer chain and N-CNTs, and made the polymer chain not easy to relax, resulting in the decrease of equilibrium swelling ratio.[44]

3.5 Conductive properties of hydrogel

The electrical conductivity of the composite hydrogel depends on the content of N-CNTs and the degree of modification. The sample were cut into 10 mm thickness at room temperature, and then the electrical conductivity of five groups of hydrogels at different time periods were recorded. Fig. 9 showed the change of electrical conductivity of five groups of samples with time within 30 hours, it could be seen from the figure that the electrical conductivity of the five groups of hydrogels increased gradually, which could be attributed to the ChCl with strong water absorption in the composite hydrogel caused the water molecules in the air to enter the gel, and the pores and water environment in the hydrogel were conducive to the rapid transfer of electrons, resulting in the change of electrical conductivity.[45] The highest conductivity of FP1, FP2, FP3 and FP4 were 0.12(±0.02), 0.15(±0.03), 0.33(±0.01) and 0.42(±0.02) mS cm^{-1} respectively, which was 1.2, 1.5, 3.3 and 4.2 times higher than that of FP0 (the highest conductivity reached 0.1 mS cm^{-1}). Three groups of hydrogels, FP0, FP2 and FP4, were connected to the circuit, and Fig. 10 showed the brightness change of the LED in the circuit before and after water absorption. It was found that the diodes connected in the circuit do not emit light before absorbing water, but all the three groups of diodes emit light after absorbing water for 30 hours, and the luminous brightness increased with the increase of N-CNTs content. The above phenomena showed that the electrical conductivity of the composite hydrogel increases with the increase of N-CNTs content, which was due to the excellent electrical conductivity of N-CNTs, and its dispersion into the hydrogel matrix could enhance the electrical properties of the hydrogel.[46] Therefore, the FP4 hydrogel with the highest N-CNTs content showed the highest conductivity, and the LED connected with FP4 hydrogel had the brightest brightness.

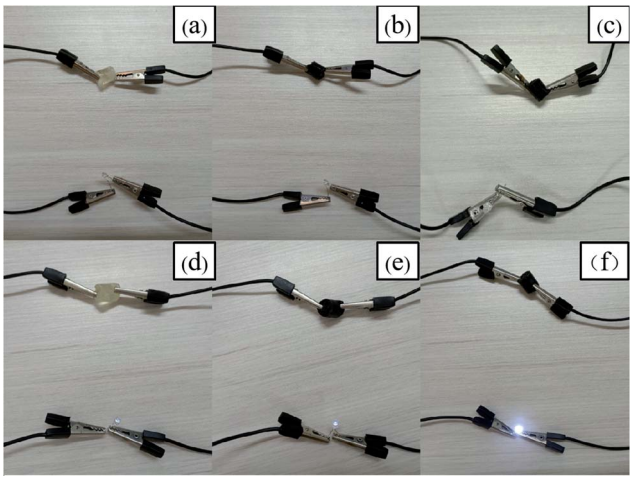

Fig. 10 Brightness change of LED connected to FP0, FP2, FP4 hydrogel circuit before and after absorbing water; (a)–(c) before absorbing water; (d)–(f) after absorbing water.

Compared with the hydrogels without or with less N-CNTs, the N-CNTs/P(AA-*co*-AM) composite hydrogels with 1 wt% N-CNTs content had the best mechanical properties and conductive effect, and the composite hydrogels showed excellent pH response properties in alkaline environment. These advantages give the composite hydrogel a wide application prospect in the fields of electronic components and biomedical materials.

4. Conclusions

Ternary DES was prepared by frontal polymerization with AM, AA and ChCl as raw materials, adding N-CNTs as filler to DES, N-CNTs/P(AA-*co*-AM) composite hydrogel was successfully prepared, the mechanical properties, pH responsiveness and electrical conductivity of the composite hydrogels were analyzed. Research shows that:

(1) Due to the strong interfacial connection between N-CNTs and macromolecules in DES, the mechanical properties of the hydrogel were significantly enhanced with the increase of N-CNTs content. The tensile strength of the composite hydrogel with 1.0 wt% N-CNTs content reached 5.42 MPa, which was 4.7 times that of the hydrogel without N-CNTs, and the compressive strength of the hydrogel was 2.08 times higher than that of the hydrogel without N-CNTs.

(2) The composite hydrogel has excellent pH response in alkaline environment, which makes N-CNTs/P(AA-*co*-AM) composite hydrogel have a certain application prospect in controlled drug release and so on.

© 2022 The Author(s). Published by the Royal Society of Chemistry

Open Access Article. Published on 29 June 2022. Downloaded on 2/6/2026 6:33:03 AM. This article is licensed under a Creative Commons Attribution-NonCommercial 3.0 Unported Licence.

(3) The composite hydrogel with 1.0 wt% N-CNTs content has the best mechanical properties, and its electrical conductivity is 4.2 times higher than that of the hydrogel without N-CNTs. The addition of N-CNTs makes up for the low mechanical properties of hydrogel in the electrical field.

Author contributions

B. L., proposed the ideas, steps and details of the experiment, most of the experiments were done by X. J. X., M. J. Z., J. Z. L., where X. J. X., was instrumental in the proper conduct of the experiments and wrote the article together with B. L., and all the authors analyzed the data, discussed the conclusions.

Conflicts of interest

The authors declare that there are no competing interests regarding the publication of this article.

Acknowledgements

The work is supported by Marine Defense Technology Innovation Center Innovation Fund (JJ-2020-719-01), Natural Science Foundation of Hubei Province (2021CFB292) and Research and Innovation Initiatives of WHPU (2022J04). This work was finished at Wuhan University of Technology (WUT) and Wuhan Polytechnic University, Wuhan.

Notes and references

1 M. Rasoulzadeh and H. Namazi, *Carbohydr. Polym.*, 2017, **168**, 320–326.
2 M. Yadollahi, S. Farhoudian and H. Namazi, *Int. J. Biol. Macromol.*, 2015, **79**, 37–43.
3 S. Li, W. Huang and X. Liu, *Chin. J. Appl. Chem.*, 2008, **25**(10), 1225–1228.
4 J. Cai, X. Zhang and W. Liu, *Polymer*, 2020, **202**, 122643.
5 X. Liang, B. Qu and J. Li, *React. Funct. Polym.*, 2015, **86**, 1–6.
6 H. X. Zhang, W. Niu and S. Zhang, *Chem. Eng. J.*, 2020, **1387**, 124105–124114.
7 W. Zheng, Y. Li and L. Xu, *Polymer*, 2020, **211**, 123095.
8 P. Pissis and A. Kyritsis, *Solid State Ionics*, 1997, **97**(1–4), 105–113.
9 E. Zygado-Monikowska, Z. Florjańczyk and E. Wielgus-Barry, *J. Power Sources*, 2006, **159**(1), 385–391.
10 W. Wieczorek and J. R. Stevens, *Polymer*, 1997, **38**(9), 2057–2065.
11 J. Przyluski, Z. Poitarzewski and W. Wieczorek, *Polymer*, 1998, **39**(18), 4343–4347.
12 X.-G. Sun, G. Liu and J. Xie, *Solid State Ionics*, 2004, **175**, 713–716.
13 J. Wu, Z. Lan and D. Wang, *Electrochim. Acta*, 2006, **51**(20), 4243–4249.
14 E. A. Moschou, S. F. Peteu and L. G. Bachas, *Chem. Mater.*, 2014, **16**(12), 2499–2502.
15 T. Dai, X. Qing and L. Yun, *Polymer*, 2009, **50**(22), 5236–5241.
16 K. S. Sivudu and K. Y. Rhee, *Colloids Surf., A*, 2009, **349**(1–3), 29–34.
17 A. Michalska, M. Wojciechowski and E. Bulska, *Talanta*, 2010, **82**(1), 151–157.
18 Z. R. Ismagilov, A. E. Shalagina and O. Y. Podyacheva, *Carbon*, 2009, **47**(8), 1922–1929.
19 J. Lin, Q. Tang and J. Wu, *React. Funct. Polym.*, 2007, **67**(4), 275–281.
20 K. Fujisawa, T. Tojo and H. Muramatsu, *Nanoscale*, 2011, **3**(10), 4359–4364.
21 Z. Yu, B. Wen and X. Y. Song, *Acta Phys. Sin.*, 2010, **59**(5), 3583–3588.
22 Z. R. Ismagilov, A. E. Shalagina and O. Y. Podyacheva, *Carbon*, 2009, **47**(8), 1922–1929.
23 J. A. Pojman, J. Willis and D. Fortenberry, *J. Polym. Sci., Part A: Polym. Chem.*, 2010, **33**(4), 643–652.
24 K. F. Fazende, M. Phachansitthi, M. Morales and D. Josué, *J. Polym. Sci.*, 2017, **55**(24), 4046–4050.
25 J. A. Pojman, G. Curtis and V. M. Ilyashenko, *J. Am. Chem. Soc.*, 1996, **118**(15), 3783–3784.
26 E. L. Smith, A. P. Abbott and K. S. Ryder, *Chem. Rev.*, 2014, **114**(21), 11060–11082.
27 J. Mota-Morales, M. C. Gutierrez and I. C. Sanchez, *Chem. Commun.*, 2011, **47**(18), 5328–5330.
28 J. D. Mota-Morales, M. C. Gutiérrez and M. L. Ferrer, *J. Polym. Sci., Part A: Polym. Chem.*, 2013, **51**(8), 1767–1773.
29 P. Abbott, G. Capper, D. L. Davies, R. K. Rasheed and V. Tambyrajah, *Chem. Commun.*, 2003, **1**, 70–71.
30 Y. Chen, S. Li and S. Yan, *Carbohydr. Polym.*, 2021, **263**, 117996.
31 S. Li and S. Yan, *RSC Adv.*, 2016, **6**(40), 33426–33432.
32 B. Li, J. Liu and D. Fu, *RSC Adv.*, 2021, **11**(56), 35268–35273.
33 Y. Meng and L. Miao, *Chem. Res. Chin. Univ.*, 2019, **35**(1), 1–8.
34 X. Hu, J. Liu and Q. He, *Nanoscale*, 2016, **8**(7), 4260.
35 Y. U. Meng and M. Liu, *Sci. Tech. Eng.*, 2019, **19**(18), 356–360.
36 Z. Li, M. Tang and J. Dai, *Polymer*, 2016, **85**, 67–76.
37 Y. Bin, *Research on the Preparation and Mechanical Properties of Carbon Nanotubes Reinforced Composites*, Dalian University of Technology, 2016.
38 X. Tong, J. Zheng and Y. Lu, *Mater. Lett.*, 2007, **61**(8–9), 1704–1706.
39 Y. Ying, Z. Jia and Y. Zeng, *Polym. Mater.: Sci. Eng.*, 2003, **19**(3), 198–200.
40 X. Ming, *Effect of carbon nanotubes on the properties of smart gels*, Tianjin University of Technology, 2006.
41 H. Dai and H. Huang, *J. Agric. Food Chem.*, 2017, **65**(3), 565–574.
42 B. Işık, *J. Appl. Polym. Sci.*, 2010, **91**(2), 1289–1293.
43 F. Lijuan, Y. Jinxiu and L. Haibo, *Mater. Sci. Forum*, 2016, **873**, 84–88.
44 L. Zhang, X. Sun and Z. Jing, *Chem. Ind. Eng. Prog.*, 2013, **32**(8), 1881–1886.
45 H. Ding, X. Liang, Q. Wang, M. Wang and G. Sun, *Carbohydr. Polym.*, 2020, **248**, 116797.
46 Y. Dong, X. Long and H. Zhou, *Journal of Asian Earth Sciences*, 2010, **39**(3), 173–191.

© 2022 The Author(s). Published by the Royal Society of Chemistry